Effects of incompressibility K_0 in heavy-ion collisions at intermediate energies

Xiao-Xiao Long[1] and Gao-Feng Wei[1,2,*]

[1]*School of Physics and Electronic Science, Guizhou Normal University, Guiyang 550025, China*

[2]*Guizhou Provincial Key Laboratory of Radio Astronomy and Data Processing, Guizhou Normal University, Guiyang 550025, China*

(Received 13 February 2024; accepted 29 April 2024; published 21 May 2024)

Within the possible least uncertainty on the nuclear incompressibility K_0, we examine effects of K_0 in heavy-ion collisions at intermediate energies. Based on simulations of Au + Au collisions at 400 MeV/nucleon using an isospin- and momentum-dependent transport model, we find that the incompressibility K_0 indeed affects significantly the attainable density in central regions, and thus the particle productions and/or distributions at final states, e.g., nucleon rapidity distributions and yields of charged pions. Nevertheless, through examining the free neutron over proton ratios n/p, the neutron-proton differential transverse and directed flows as well as the charged pion ratio π^-/π^+ and its kinetic energy distribution, we find that these observables are less affected by the uncertainty of K_0, but mainly sensitive to the slope of symmetry energy at the saturation density. We also compare and discuss our results with the corresponding data.

DOI: 10.1103/PhysRevC.109.054619

I. INTRODUCTION

As one of the central issues in isospin nuclear physics, the symmetry energy $E_{\mathrm{sym}}(\rho)$ at suprasaturation densities has been a longstanding interest due to its importance in understanding the properties of radioactive nuclei and evolution of supernova and neutron stars [1–7]. In terrestrial laboratories, heavy-ion collisions (HICs) with rare isotopes provide a unique opportunity to generate directly the isospin asymmetric nuclear matter at high densities, and thus enable one to extract the information about the $E_{\mathrm{sym}}(\rho)$ at high densities through comparing the theoretical simulations of isospin observables with the corresponding data [8–11].

The incompressibility K_0 of nuclear matter at the saturation density ρ_0, as an important input of most microscopic and/or phenomenological heavy-ion transport models, affects the attainable density in collision regions and thus the particle productions and/or distributions at final states. Naturally, the accuracy of K_0 affects the quantitative extraction of the symmetry energy using HIC models. However, the possibly tightest constraint or least uncertainty one currently obtains on the K_0 is 230 ± 30 MeV [12–17]. This uncertainty on the value of K_0 naturally prevents one from quantitatively extracting the high density symmetry energy information using isospin observables. Actually, some literatures have already involved in investigations of the uncertainty of K_0 in HICs and other aspects. For example, using a Tübingen quantum molecular dynamics model, Ref. [18] discussed effects of K_0 within a range from 210 to 280 MeV on the nucleon elliptic flows, and Ref. [19] examined effects of K_0 within a range from 195 to 225 MeV on the nucleus-nucleus dynamic potential in fusion reactions, and Ref. [20] studied effects of K_0 within a range from 210 to 240 MeV on the giant resonances in ^{40,48}Ca, ^{68}Ni, ^{90}Zr, ^{116}Sn, ^{144}Sm, and ^{208}Pb. Nevertheless, a systematical study related to the effects of K_0 on the symmetry energy observables is rarely reported. On the other hand, it is well known that central heavy-ion reactions at intermediate energies play a special role in determination of the symmetry energy especially above two times the saturation density. Therefore, it is naturally necessary to study effects of K_0 in central heavy-ion reactions at intermediate energies. To this end, we perform a central Au + Au collision at 400 MeV/nucleon to study effects of K_0 within the possible tightest constraint, i.e., $K_0 = 230 \pm 30$ MeV, on the pion and nucleon observables. It is shown that the K_0 indeed affects significantly the attainable density in collision regions, and thus the particle productions at final states, e.g., charged pion multiplicities, etc. However, we find that the free neutron over proton ratios n/p, the neutron-proton differential transverse and directed flows as well as the charged pion ratio π^-/π^+ and its kinetic energy distribution could reduce significantly the effects of uncertainties of K_0 and thus show more sensitivities to the high density behavior of symmetry energy.

In the following, we first describe briefly the used isospin- and momentum-dependent Boltzmann-Uehling-Uhlenbeck transport model (IBUU) [21,22] in Sec. II. We then discuss our results in Sec. III. A summary will be given in Sec. IV.

II. THE MODEL

The present study is carried out within an updated version of the IBUU transport model [23]. In this version, we adopt a separate density-dependent scenario [24] for a more delicate treatment of the in-medium many-body force effects as in Refs. [25,26]. Also, we introduce a parameter z [27] as in Ref. [28] to mimic the value of $E_{\mathrm{sym}}(\rho)$ at ρ_0 and $\tilde{\rho} \approx 2\rho_0/3$ to meet the best knowledge of $E_{\mathrm{sym}}(\rho)$ at the two

*Corresponding author: wei.gaofeng@gznu.edu.cn

densities one has obtained so far, e.g., $E_{\rm sym}(\rho_0) = 32.5 \pm 2$ MeV [18], 32.5 ± 3.2 MeV [29], $33.0^{+2}_{-1.8}$ MeV [30], 38.3 ± 4.7 MeV [31], 35.3 ± 2.8 MeV [32], and $E_{\rm sym}(\tilde{\rho} = 0.1\,{\rm fm}^{-3}) = 25.5 \pm 1$ MeV [33], $E_{\rm sym}(\tilde{\rho} = 0.11\,{\rm fm}^{-3}) = 26.2 \pm 1$ MeV [34], $E_{\rm sym}(\tilde{\rho} = 0.11\,{\rm fm}^{-3}) = 26.65 \pm 0.2$ MeV [35]. As to the high density behavior of $E_{\rm sym}(\rho)$, we use the parameter x to control the slope value $L \equiv 3\rho(dE_{\rm sym}/d\rho)$ of $E_{\rm sym}(\rho)$ at ρ_0 as in the original IBUU model [21,22]. All of these features have been incorporated into the presently used model, see Ref. [23] for details. Specifically, the isospin and momentum dependent nuclear interaction (MDI) used is expressed as

$$\begin{aligned} U(\rho, \delta, \vec{p}, \tau) &= A_u \frac{\rho_{-\tau}}{\rho_0} + A_l \frac{\rho_\tau}{\rho_0} + \frac{B}{2}\left(\frac{2\rho_\tau}{\rho_0}\right)^{\sigma}(1-x) \\ &+ \frac{2B}{\sigma+1}\left(\frac{\rho}{\rho_0}\right)^{\sigma}(1+x)\frac{\rho_{-\tau}}{\rho}\left[1+(\sigma-1)\frac{\rho_\tau}{\rho}\right] \\ &+ \frac{2C_l}{\rho_0}\int d^3p' \frac{f_\tau(\vec{p}')}{1+(\vec{p}-\vec{p}')^2/\Lambda^2} \\ &+ \frac{2C_u}{\rho_0}\int d^3p' \frac{f_{-\tau}(\vec{p}')}{1+(\vec{p}-\vec{p}')^2/\Lambda^2}, \end{aligned} \tag{1}$$

where $\tau = 1$ for neutrons and -1 for protons, and A_u, A_l, $C_u(\equiv C_{\tau,-\tau})$ and $C_l(\equiv C_{\tau,\tau})$ are expressed as

$$\begin{aligned} A_l &= A_{l0} + U^{\infty}_{\rm sym}(\rho_0) - \frac{2B}{\sigma+1} \\ &\quad \times \left[\frac{(1-x)}{4}\sigma(\sigma+1) - \frac{1+x}{2}\right], \\ A_u &= A_{u0} - U^{\infty}_{\rm sym}(\rho_0) + \frac{2B}{\sigma+1} \\ &\quad \times \left[\frac{(1-x)}{4}\sigma(\sigma+1) - \frac{1+x}{2}\right], \\ C_l &= C_{l0} - 2\big(U^{\infty}_{\rm sym}(\rho_0) - 2z\big)\frac{p^2_{f0}}{\Lambda^2 \ln\left[\left(4p^2_{f0}+\Lambda^2\right)/\Lambda^2\right]}, \\ C_u &= C_{u0} + 2\big(U^{\infty}_{\rm sym}(\rho_0) - 2z\big)\frac{p^2_{f0}}{\Lambda^2 \ln\left[\left(4p^2_{f0}+\Lambda^2\right)/\Lambda^2\right]}. \end{aligned}$$

The eight parameters embedded in the above expressions, i.e., A_{l0}, A_{u0}, B, σ, C_{l0}, C_{u0}, Λ, and z, are determined by fitting eight experimental and/or empirical constraints on properties of nuclear matter at $\rho_0 = 0.16$ fm^{-3}. Among them, the first seven are the binding energy -16 MeV, the pressure $P_0 = 0$ MeV/fm^3, the isoscalar effective mass $m^*_s = 0.7m$, the isoscalar potential at infinitely large nucleon momentum $U^{\infty}_0(\rho_0) = 75$ MeV, the isovector potential at infinitely large nucleon momentum $U^{\infty}_{\rm sym}(\rho_0) = -100$ MeV, and the $E_{\rm sym}(\rho)$ at ρ_0 and $\tilde{\rho} \approx 2\rho_0/3$. The eighth is K_0 that we are going to examine. To this end, we take three values for K_0 within the possible least uncertainty as aforementioned in this study, i.e., 200, 230, and 260 MeV. For these different settings of K_0, the corresponding values of A_{l0}, A_{u0}, B, and σ are shown in Table I, and the values of C_{l0}, C_{u0}, and Λ are $C_{l0} = -60.486$ MeV, $C_{u0} = -99.702$ MeV, and $\Lambda = 2.424p_{f0}$, where p_{f0} refers to the nucleon Fermi momentum in symmetric nuclear matter (SNM) at ρ_0. Also, to make the symmetry energy observable more clearly reflecting effects of K_0, we adjust the values of x and z for different K_0 settings to ensure the identical slope L of $E_{\rm sym}(\rho)$ at ρ_0 as shown in Fig. 1. In addition, for a certain K_0, we also take four different settings for L, and to enable us to compare effects of K_0 and L on the symmetry energy observables. It should be mentioned that the parameter z should ensure the values of symmetry energy at both ρ_0 and $\tilde{\rho} \approx 2\rho_0/3$ to be basically within the allowed ranges as indicated in Refs. [18,29–35] as aforementioned. In this study, we limit the value of symmetry energy at $\tilde{\rho} \approx 2\rho_0/3$ within the range of 25.5 ± 1 MeV, while that at ρ_0 is determined as $E_{\rm sym}(\rho_0) = 32.5 + z$ MeV. The specific values of x and z and the corresponding L as well as the $E_{\rm sym}(2\rho_0/3)$ are shown in Table II.

TABLE I. The values of A_{l0}, A_{u0}, B, σ, and the resulting K_0.

$A_{l0} = A_{u0}$ (MeV)	B (MeV)	σ	K_0 (MeV)
−455.726	530.726	1.0646	200
−66.963	141.963	1.2652	230
−12.992	87.992	1.4657	260

III. RESULTS AND DISCUSSIONS

Now, we present the results of Au+Au collisions at 400 MeV/nucleon with an impact parameter of $b = 0$–2 fm, corresponding to a typical reaction with a reduced impact parameter of $b_0 \leqslant 0.15$ at 400 MeV/nucleon carried out at the FOPI detector [36–38].

A. Nucleon observables

Shown in Fig. 2 are the evolutions of reduced average densities in central spherical regions with a radius of 2 fm.

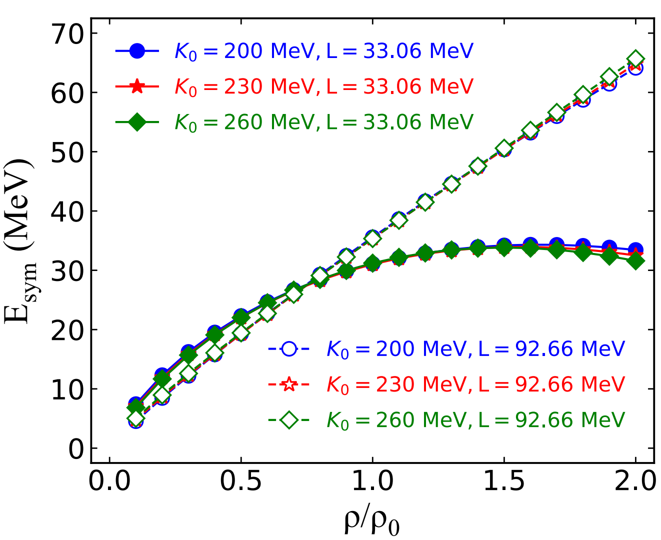

FIG. 1. Density dependence of the $E_{\rm sym}(\rho)$ with different K_0 and L.

TABLE II. The values of x, z and the resulting K_0, L, and $E_{\mathrm{sym}}(2\rho_0/3)$.

K_0 (MeV)	x	z (MeV)	L (MeV)	$E_{\mathrm{sym}}(2\rho_0/3)$ (MeV)
200	0.54	−1.408	33.06	26.06
200	0.08	0.474	61.95	25.24
200	−0.38	3.066	92.66	24.93
200	−0.84	5.8	123.73	24.71
230	0.6	−1.482	33.06	25.90
230	0.2	0.326	61.95	25.10
230	−0.2	2.844	92.66	24.80
230	−0.6	5.505	123.73	24.60
260	0.66	−1.3	33.06	25.98
260	0.31	0.418	61.95	25.18
260	−0.04	2.845	92.66	24.88
260	−0.39	5.415	123.73	24.67

To study how the K_0 and L affect the attainable compression densities in the reactions, we take six different combinations of K_0 and L in simulations of Au + Au collisions. It is seen that, for a certain L, the compression density reached in central regions is significantly larger with a smaller value of K_0 than that with a larger one; while for a certain K_0, the compression density reached is significantly larger with a soft symmetry energy (i.e., a smaller slope value L) than that with a stiff one (i.e., a larger slope value L). These observations are exactly the features belonging to HICs at intermediate energies [8,10] since the effect of symmetry energy on the compression density is decreasing even to a negligible degree as the beam energy increases up to approximately 1 GeV and above [23]. However, if one compares semiquantitatively effects between K_0 and L on the compression density, e.g., varying K_0 from 260 to 200 MeV and L from 92.66 to 33.06 MeV, their relative changes are $(260-200)/[(260+200)/2] \times \% \approx 26\%$ and $(92.66-33.06)/[(92.66+33.06)/2] \times \% \approx 94.8\%$, one can explicitly find from Fig. 2 that the effect of K_0 on the compression density is obviously more dominant than that of L, reflecting the fact that the nuclear compression is overall dominated by the bulk equation of state (EoS) of nuclear matter. Naturally, one expects that these features could be reflected by the nucleon observables at final states. To this end, we show in Fig. 3 the rapidity distributions of free neutrons and protons at final states, where the criterion of free nucleons is defined as the relative distances $\Delta_R > 3.575$ fm or momenta $\Delta_p > 0.3$ GeV/c as in coalescence models [39–43]. It is seen that, for a certain L, both the free neutrons and protons are greater with a larger K_0 than those with a smaller K_0 as shown in the insets, since the isoscalar potentials have approximately identical effects on neutrons and protons. While for a certain K_0, it is obvious to see that the variation tendency of neutrons is completely opposite to that of protons when varying the L, reflecting the fact that the symmetry potential/energy has opposite effects on neutrons and protons at high densities, i.e., repulsion on neutrons but attraction on protons. To these observations, one naturally expects the

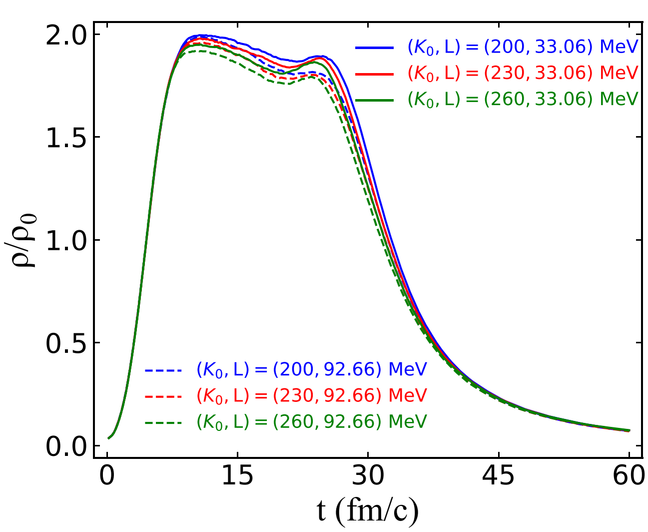

FIG. 2. Evolution of reduced average densities ρ/ρ_0 in central spherical regions with a radius of 2 fm in Au+Au collisions at 400A MeV with different K_0 and L.

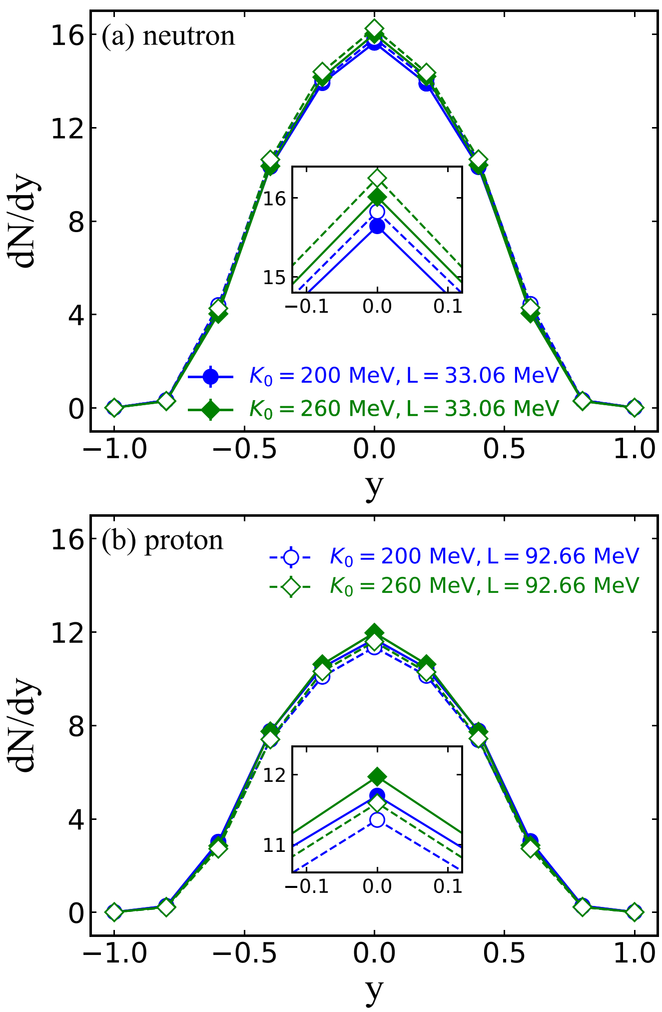

FIG. 3. Rapidity distributions of neutrons (a) and protons (b) in Au+Au collisions at 400A MeV with different combinations of K_0 and L.

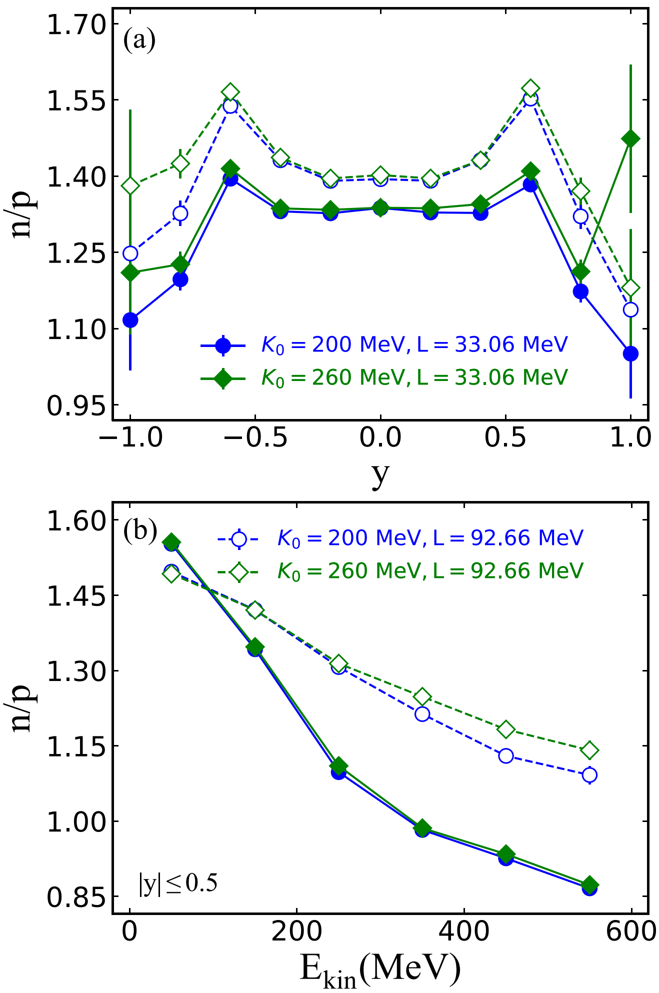

FIG. 4. Rapidity (a) and kinetic energy (b) distributions of n/p ratios in Au+Au collisions at 400A MeV with different combinations of K_0 and L.

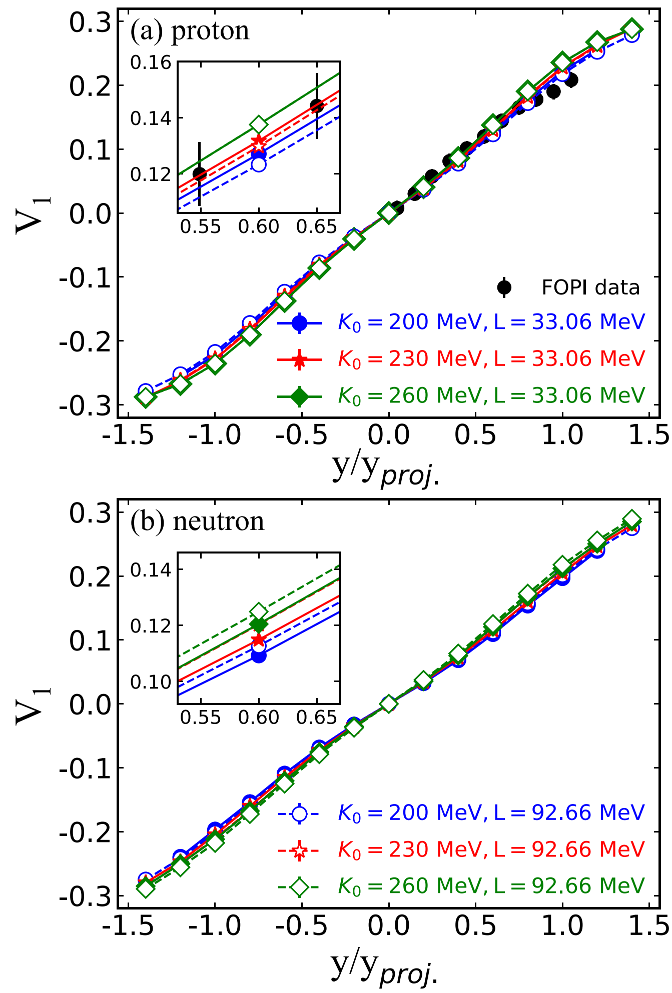

FIG. 5. Directed flows of protons (a) and neutrons (b) in Au+Au collisions at 400 MeV/nucleon with different combinations of K_0 and L.

ratios of free neutrons over protons could reduce the isoscalar potential effects and enlarge the symmetry potential/energy effects.

Shown in Fig. 4(a) are the rapidity distributions of neutrons over protons n/p with different combinations of K_0 and L. As one expected, the n/p ratios indeed significantly reduce effects of K_0 and enlarge those of L. Moreover, because nucleons at midrapidities are mainly from early emissions during the compression stage, and thus carry the information of symmetry energy at high densities. Therefore, we can observe a larger n/p ratio with a stiff symmetry energy than that with a soft one. Similarly, it is seen that the kinetic energy distributions of n/p ratios at midrapidities are mainly sensitive to the high density behavior of symmetry energy as shown in Fig. 4(b).

B. Flow observables

Collective motions of final state nucleons are the direct reflections of the pressure created in HICs and thus are closely related to the equation of state of dense nuclear matter. Therefore, in this subsection, we examine how the K_0 and L affect the collective motions of final state nucleons. In our studied reactions, the main collective motions could be reflected by the directed flows v_1 and/or transverse flows p_x. Shown in Fig. 5 are the rapidity dependent directed flows of free neutrons and protons at final states. The insets are a local amplification to explicitly show effects of K_0 and L. To compare with the corresponding FOPI data [36–38], we use the same reduced rapidity as in Refs. [36–38], i.e., $y/y_{\mathrm{proj.}}$. First, it is seen that our results are consistent with the data. Second, similar to the observations in rapidity distributions of neutrons and protons shown in Fig. 3, the effects of symmetry energy/potential are completely opposite for neutrons and protons, while the effects of K_0 on neutrons and protons are approximately identical. Therefore, we turn to the free neutron-proton differential directed and transverse flows defined as [8,27,44,45]

$$v_1^{np} = \frac{N_n(y)}{N(y)}\langle v_1^n(y)\rangle - \frac{N_p(y)}{N(y)}\langle v_1^p(y)\rangle, \tag{2}$$

$$p_x^{np} = \frac{N_n(y)}{N(y)}\langle p_x^n(y)\rangle - \frac{N_p(y)}{N(y)}\langle p_x^p(y)\rangle, \tag{3}$$

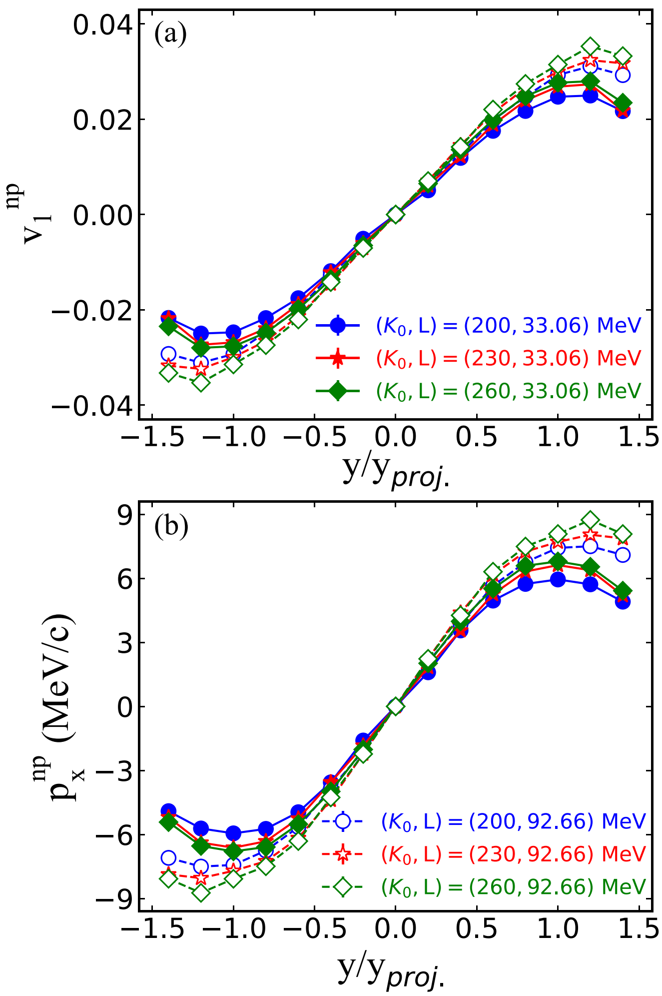

FIG. 6. Free neutron-proton differential directed (a) and transverse (b) flows in Au+Au collisions at 400 MeV/nucleon with different combinations of K_0 and L.

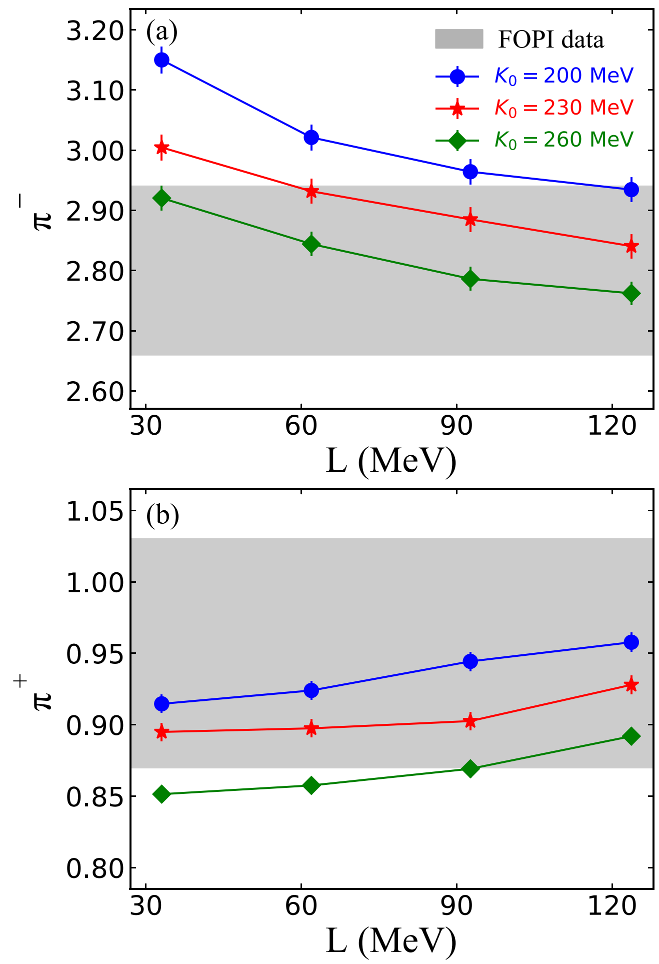

FIG. 7. Multiplicities of π^- (a) and π^+ (b) in Au+Au collisions at 400 MeV/nucleon with different combinations of K_0 and L.

where $N_n(y)$, $N_p(y)$, and $N(y)$, respectively, represent the total number of free neutrons, protons, and nucleons at rapidities y. Shown in Fig. 6 are the corresponding simulations of free neutron-proton differential directed v_1^{np} and transverse p_x^{np} flows. One can see that both the v_1^{np} and p_x^{np} indeed reduce significantly the effects of K_0 and show more sensitivities to the symmetry energy/potential.

C. Pion observables

In HICs at intermediate energies, pions are produced mostly from the decay of $\Delta(1232)$ resonances. Specifically, for the charged pions, the main channels are $\Delta^- \leftrightarrow n + \pi^-$ and $\Delta^{++} \leftrightarrow p + \pi^+$. On the other hand, the main channels of producing Δ^- and Δ^{++} from nucleon-nucleon collisions at high densities are $nn \rightarrow p + \Delta^-$ and $pp \rightarrow n + \Delta^{++}$. Equivalently, one can view the production of π^- as mainly from inelastic $nn \rightarrow pn\pi^-$ channels while that of π^+ mainly from $pp \rightarrow pn\pi^+$ channels. This is why the ratio π^-/π^+ is sensitive to the high density behavior of nuclear symmetry energy in HICs.

Shown in Fig. 7 are the multiplicities of π^- and π^+ in Au+Au collisions at 400 MeV/nucleon with different combinations of K_0 and L. First, it can be observed that, consistent with the previous observations using most transport models, the yields of π^- and π^+ are sensitive to L, and the sensitivity of π^- is greater than that of π^+. Moreover, the variation tendency of π^- with L is opposite to that of π^+ similar to that of nucleons. At the same time, we can find that yields of both π^- and π^+ are also sensitive to K_0. More specifically, both π^- and π^+ are more produced in collisions with a smaller K_0 due to a larger compression formed in collisions as shown in Fig. 2. To this observation, one naturally expects that the ratio π^-/π^+ could reduce significantly the effects of K_0 and thus show more sensitivities to the high density behavior of symmetry energy. Indeed, this can be demonstrated by the total π^-/π^+ ratios and the kinetic energy distributions as shown in Fig. 8. In addition, we also show the corresponding data in Figs. 7 and 8. It can be found that extracting the information of high density symmetry energy from multiplicities of both π^- and π^+ depends seriously on the used K_0, while that from both total π^-/π^+ ratio and its kinetic energy distributions is free of uncertainties of K_0.

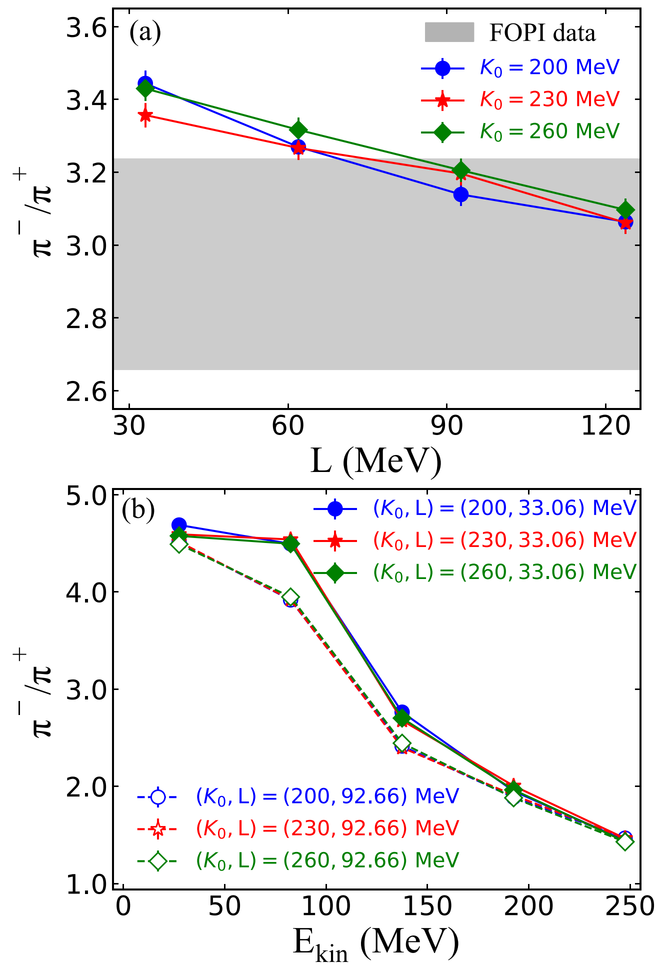

FIG. 8. Ratios π^-/π^+ as a function of L (a) and pion kinetic energy (b) in Au+Au collisions at 400 MeV/nucleon with different combinations of K_0 and L.

Before ending this part, we give a useful remark on the kinetic energy distributions of π^-/π^+ ratios. We note that our π^-/π^+ ratio at high kinetic energies is insensitive to the symmetry energy, while in the study on subthreshold pion production from the pBUU [46] model it appears that the π^-/π^+ ratio at high kinetic energies is still and even more sensitive to the symmetry energy, and a soft symmetry energy corresponds to a large π^-/π^+ ratio. Moreover, we find from the spectral pion ratio simulated with the dcQMD model [32] that the sensitivity of π^-/π^+ ratio to the symmetry energy will cross as the transverse momenta of pions increase, i.e., for pions with the low transverse momenta, the π^-/π^+ ratio is large with a soft symmetry energy, but for pions with the high transverse momenta, the opposite is true. It appears that the sensitivity of π^-/π^+ ratio at high kinetic energies or high transverse momenta is still uncertain and needs to be further studied. The discrepancies of π^-/π^+ ratios at high kinetic energies and/or transverse momenta might originate from the different Δ potential that affects the decay of Δ and thus the attainable kinetic energy for pions. Another possibility is the pion potential that affects the propagation of pions in nuclear medium and thus the kinetic energy distributions of pions at final states. Therefore, it will be interesting to see how these factors affect the kinetic energy distributions of π^-/π^+ ratios, especially at high kinetic energies.

IV. SUMMARY

In summary, we have studied the effects of incompressibility K_0 within its possible least uncertainty in HICs at intermediate energies. It is shown that the K_0 indeed affects significantly the attainable density in central collision regions, and thus the particle productions and/or distributions at final states, e.g., nucleon rapidity distributions and yields of charged pions. However, considering that the effects of K_0 on neutrons and protons are approximately identical, we have examined and found that the free neutron over proton ratios n/p, the neutron-proton differential transverse p_x^{np}, and directed v_1^{np} flows could reduce significantly effects of K_0 and thus show more sensitivities to the symmetry energy. Similarly, the π^-/π^+ ratio and its kinetic energy distributions are also found to be less affected by the uncertainty of K_0, but mainly sensitive to the slope of symmetry energy at ρ_0.

ACKNOWLEDGMENTS

This work is supported by the National Natural Science Foundation of China under Grants No. 11965008 and No. 11405128, and Guizhou Provincial Science and Technology Foundation under Grant No. [2020]1Y034, and the PhD-funded project of Guizhou Normal University (Grant No. GZNUD[2018]11).

[1] A. W. Steiner, M. Prakash, J. M. Lattimer, and P. J. Ellis, Phys. Rep. **411**, 325 (2005).
[2] J. M. Lattimer, Annu. Rev. Nucl. Part. Sci. **62**, 485 (2012).
[3] C. J. Horowitz, E. F. Brown, Y. Kim, W. G. Lynch, R. Michaels, A. Ono, J. Piekarewicz, M. B. Tsang, and H. H. Wolter, J. Phys. G: Nucl. Part. Phys. **41**, 093001 (2014).
[4] K. Hebeler, J. D. Holt, J. Menéndez, and A. Schwenk, Annu. Rev. Nucl. Part. Sci. **65**, 457 (2015).
[5] M. Baldo and G. F. Burgio, Prog. Part. Nucl. Phys. **91**, 203 (2016).
[6] M. Oertel, M. Hempel, T. Klähn, and S. Typel, Rev. Mod. Phys. **89**, 015007 (2017).
[7] I. Tews, J. Margueron, and S. Reddy, Phys. Rev. C **98**, 045804 (2018).
[8] V. Baran, M. Colonna, V. Greco, and M. Di Toro, Phys. Rep. **410**, 335 (2005).
[9] E. E. Kolomeitsev, C. Hartnack, H. W. Barz, M. Bleicher, E. Bratkovskaya, W. Cassing, L. W. Chen, P. Danielewicz, C. Fuchs, T. Gaitanos, C. M. Ko, A. Larionov, M. Reiter, G. Wolf, and J. Aichelin, J. Phys. G: Nucl. Part. Phys. **31**, S741 (2005).

[10] B. A. Li, L. W. Chen, and C. M. Ko, Phys. Rep. **464**, 113 (2008).
[11] W. G. Lynch, M. B. Tsang, Y. Zhang, P. Danielewicz, M. Famiano, Z. Li, and A. W. Steiner, Prog. Part. Nucl. Phys. **62**, 427 (2009)
[12] C. Sturm, I. Böttcher, M. Dębowski, A. Förster, E. Grosse, P. Koczoń, B. Kohlmeyer, F. Laue, M. Mang, L. Naumann, H. Oeschler, F. Pühlhofer, E. Schwab, P. Senger, Y. Shin, J. Speer, H. Ströbele, G. Surówka, F. Uhlig, A. Wagner *et al.*, Phys. Rev. Lett. **86**, 39 (2001).
[13] C. Fuchs, A. Faessler, E. Zabrodin, and Y. M. Zheng, Phys. Rev. Lett. **86**, 1974 (2001).
[14] P. Danielewicz, R. Lacey, and W. G. Lynch, Science **298**, 1592 (2002).
[15] C. Hartnack, H. Oeschler, and J. Aichelin, Phys. Rev. Lett. **96**, 012302 (2006).
[16] Q. Pan and P. Danielewicz, Phys. Rev. Lett. **70**, 2062 (1993).
[17] J. M. Zhang, S. Das Gupta, and C. Gale, Phys. Rev. C **50**, 1617 (1994).
[18] M. D. Cozma, Eur. Phys. J. A **54**, 40 (2018).
[19] V. Zanganeh, N. Wang, and O. N. Ghodsi, Phys. Rev. C **85**, 034601 (2012).
[20] G. Bonasera, M. R. Anders, and S. Shlomo, Phys. Rev. C **98**, 054316 (2018).
[21] B. A. Li, C. B. Das, S. Das Gupta, and C. Gale, Phys. Rev. C **69**, 011603(R) (2004).
[22] B. A. Li, C. B. Das, S. Das Gupta, and C. Gale, Nucl. Phys. A **735**, 563 (2004).
[23] H. Du, G. F. Wei, and G. C. Yong, Phys. Lett. B **839**, 137823 (2023).
[24] G. F. Wei, C. Xu, W. Xie, Q. J. Zhi, S. G. Chen, and Z. W. Long, Phys. Rev. C **102**, 024614 (2020).
[25] C. Xu and B. A. Li, Phys. Rev. C **81**, 044603 (2010).
[26] L. W. Chen, C. M. Ko, B. A. Li, C. Xu, and J. Xu, Eur. Phys. J. A **50**, 29 (2014).
[27] X. Huang, G. F. Wei, Q. J. Zhi, Y. C. Yang, and Z. W. Long, Phys. Rev. C **106**, 014604 (2022).
[28] J. Xu, L. W. Chen, and B. A. Li, Phys. Rev. C **91**, 014611 (2015).
[29] R. Wang, L. W. Chen, and Y. Zhou, Phys. Rev. C **98**, 054618 (2018).
[30] R. Essick, I. Tews, P. Landry, and A. Schwenk, Phys. Rev. Lett. **127**, 192701 (2021).
[31] B. T. Reed, F. J. Fattoyev, C. J. Horowitz, and J. Piekarewicz, Phys. Rev. Lett. **126**, 172503 (2021).
[32] J. Estee, W. G. Lynch, C. Y. Tsang *et al.* (SπRIT Collaboration), Phys. Rev. Lett. **126**, 162701 (2021).
[33] B. A. Brown, Phys. Rev. Lett. **111**, 232502 (2013).
[34] N. Wang, L. Ou, and M. Liu, Phys. Rev. C **87**, 034327 (2013).
[35] Z. Zhang and L. W. Chen, Phys. Lett. B **726**, 234 (2013).
[36] W. Reisdorf, M. Stockmeier, A. Andronic *et al.* (FOPI Collaboration), Nucl. Phys. A **781**, 459 (2007).
[37] W. Reisdorf, A. Andronic, R. Averbeck *et al.* (FOPI Collaboration), Nucl. Phys. A **848**, 366 (2010).
[38] W. Reisdorf, Y. Leifels, A. Andronic *et al.* (FOPI Collaboration), Nucl. Phys. A **876**, 1 (2012).
[39] M. Gyulassy, K. Frankel, and E. A. Remler, Nucl. Phys. A **402**, 596 (1983).
[40] J. Aichelin, A. Rosenhauer, G. Peilert, H. Stoecker, and W. Greiner, Phys. Rev. Lett. **58**, 1926 (1987).
[41] V. Koch, B. Blättel, W. Cassing, U. Mosel, and K. Weber, Phys. Lett. B **241**, 174 (1990).
[42] J. L. Nagle, B. S. Kumar, D. Kusnezov, H. Sorge, and R. Mattiello, Phys. Rev. C **53**, 367 (1996).
[43] R. Scheibl and U. Heinz, Phys. Rev. C **59**, 1585 (1999).
[44] B. A. Li, Phys. Rev. Lett. **85**, 4221 (2000).
[45] B. A. Li, Phys. Rev. Lett. **88**, 192701 (2002).
[46] J. Hong and P. Danielewicz, Phys. Rev. C **90**, 024605 (2014).